

Comparison of model-simulated tropospheric NO₂ over China with GOME-satellite data

Jianzhong Ma^{a,*}, Andreas Richter^b, John P. Burrows^b, Hendrik Nüß^b,
John A. van Aardenne^{c,1}

^aKey Laboratory for Atmospheric Chemistry, Centre for Atmosphere Watch and Services, Chinese Academy of Meteorological Sciences, CMA, Beijing 100081, China

^bInstitute of Environmental Physics, University of Bremen, Otto-Hahn-Allee 1, D-28359 Bremen, Germany

^cDepartment of Atmospheric Chemistry, Max Planck Institute for Chemistry, Postfach 3060, D-55020 Mainz, Germany

Received 23 March 2005; received in revised form 2 September 2005; accepted 7 September 2005

Abstract

Tropospheric NO₂ column densities over China simulated with a regional model using different emission inventory input are compared with Global Ozone Monitoring Experiment (GOME) satellite data. These emission inventories include (i) emission estimates for the year 1995 from the Emission Database for Global Atmospheric Research (EDGAR), (ii) regional emission inventory used in the Transport and Chemical Evolution over the Pacific (TRACE-P) program with emission estimates for the year 2000 and (iii) national emission inventory used in the Chinese Ozone Research Programme (CORP) with emission estimates for the year 1995. Model simulations were performed for a summertime period and the results under clear-sky conditions were selected for comparison with GOME data of the years 1996 and 2000. The model generally reproduces high tropospheric NO₂ column densities in polluted areas of China that have been observed by GOME. However, the model simulations do not agree with the GOME measurements in a quantitative sense for some regions. Region-to-region comparisons show that with all the emission inventories the model underestimates the tropospheric NO₂ column density in remote and rural areas of China. It is found that TRACE-P underestimates the tropospheric NO₂ column density in all the regions with respect to the GOME measurements (by more than 50%). CORP and EDGAR appear to behave well for the model simulations in the North of China (within 15% deviations), but poorer for the model simulations in other regions (within 30–80% deviations). Linear regressions were performed with the NO₂ column densities available from GOME, Y , and the model, X , of each grid cell in selected regions. For all the region of China, comparison statistics are $Y = 0.361 \times X + 0.935$ with $r^2 = 0.360$ and bias = -41% for EDGAR, $Y = 1.124 \times X + 0.920$ with $r^2 = 0.472$ and bias = -67% for TRACE-P, and $Y = 0.431 \times X + 0.835$ with $r^2 = 0.509$ and bias = -31% for CORP.

© 2005 Elsevier Ltd. All rights reserved.

Keywords: Tropospheric NO₂; Emission inventory; Regional model; Satellite data; Gome; China

*Corresponding author. Fax: +86 10 6217 6414.

E-mail address: mjz@cams.cma.gov.cn (J. Ma).

¹Present address: Joint Research Centre, Institute for Environment and Sustainability, Climate Change Unit, TP280 I-21020, Ispra (V), Italy.

1. Introduction

Nitrogen dioxide (NO₂) plays a key role in the chemistry of the atmosphere. It participates in the

control of the strong oxidant, O₃, and the strongest atmospheric oxidizing agent, OH, which determine the oxidizing capacity of the atmosphere (Crutzen, 1979; Logan et al., 1981; Thompson, 1992; Lelieveld et al., 2004). Recently, it has been recognized that NO₂ contributes both directly and indirectly to the radiative forcing of climate (Solomon et al., 1999; Velders et al., 2001). In addition, NO₂ is known to cause respiratory problems for humans in the urban atmosphere (Environmental Protection Agency (EPA), 2000), and may impact the biogeochemical cycling of nitrogen in marine and coastal ecosystems by changing HNO₃ deposition in the ocean basins (Bey et al., 2001).

Nitrogen oxides (NO_x = NO + NO₂) have natural sources such as the production by lightning and microbiological processes in soils, as well as anthropogenic sources, especially fossil fuel combustion and biomass burning (Lee et al., 1997; Bradshaw et al., 2000). Although NO is produced exceptionally or predominantly from all these sources, it can be converted to NO₂ mainly by its reaction with O₃. During daytime the NO–NO₂ cycling in the troposphere occurs on a time scale of a few minutes, which is sufficiently short to establish a photostationary state between these species (Parrish et al., 1986; Ridley et al., 1992). The sum of NO and NO₂ remains more or less constant during this cycle. Global total NO_x emissions are increasing, with the most rapid increase being in Asia (by about 4–6% per year) and China and India being the largest contributors (Kato and Akimoto, 1992; Garg et al., 2001; Streets and Waldhoff, 2000; van Aardenne et al., 1999; Richter et al., 2005). However, our basic understanding of tropospheric NO_x over Asia is limited due to the lack of observations with sufficient spatial and temporal resolution. Moreover, there are still great uncertainties in the estimate of NO_x emissions in Asia (Ma and van Aardenne, 2004).

Measurements of the global distribution of NO₂ columns have become available with the Global Ozone Monitoring Experiment (GOME) (Burrows et al., 1999) which was launched in April 1995. The NO₂ maps derived from these measurements have been used to study the NO₂ fields on both global and regional scales (e.g. Burrows et al., 1999; Leue et al., 2001; Richter and Burrows, 2002; Martin et al., 2002; Edwards et al., 2003; Beirle et al., 2003; Schaub et al., 2005). Although the satellite instrument provides measurements of the integrated tropospheric column of NO₂, the values are

dominated by the amounts in the lower troposphere as a result of the relatively short lifetime of NO_x.

The GOME tropospheric NO₂ columns reveal “hotspots” of significance for the assessment of regional, transnational and intercontinental air pollution. Comparison of the model output to the GOME data illustrates the degree to which present models reproduce the hot spots seen in the GOME data. In turn, the comparison of simulated NO₂ columns and those derived from satellite measurements may be helpful for evaluation of the satellite measurement derived data, taking into account that the procedure of retrieval of tropospheric NO₂ columns from satellite measurements always involves some priori assumptions which are difficult to validate.

GOME data have been used to evaluate global and regional models in their capability of simulating tropospheric NO₂ (e.g., Velders et al., 2001; Lauer et al., 2002; Kunhikrishnan et al., 2004; Kononov et al., 2005), and to retrieve the NO_x emissions (Martin et al., 2003; Müller and Stavrakou, 2005). The geographical distribution pattern and seasonal variation of the GOME tropospheric NO₂ columns are generally reproduced with the models. However, the quantitative comparison is limited both by the uncertainty in the tropospheric NO₂ columns derived from GOME caused by the uncertainty, e.g., in the air mass factors and cloud cover, and by the quality of model performance in the simulation of major chemical and transport processes that are related to NO₂ variations in spatial and temporal scales. Although the NO_x emission data used have been recognized as one of the most important uncertainties in the models, the influence of using different emission databases on the comparison of simulated NO₂ columns and the GOME data has not been well addressed to our knowledge.

In this paper we present the difference in simulated tropospheric NO₂ columns over China due to the use of different emission inventories in a regional model, and compare these tropospheric NO₂ columns with those retrieved from GOME measurements. In the next section, the model along with the three emission inventories used and the GOME retrieval technique are briefly described. Following that in Section 3, the model simulations are compared with GOME NO₂ observations, and the sensitivity of model results to the selected parameter is tested. Conclusions and remarks are given in Section 4. The present study is the first examination of tropospheric NO₂ over China

applying the combination of satellite tropospheric NO₂ column data together with a regional model with different emission inventory input.

2. Methodology

2.1. Model description

The model used in this study is a 3-D regional chemical transport model (Ma et al., 2002a), which is extended from the regional acid deposition model (RADM) and aimed at studying the distribution and budget of tropospheric ozone and its precursors over China. The model domain covers China with a horizontal resolution of 100 km. In the vertical, the model extends up to pressure levels of 10 mbar for meteorological simulations and to the local thermal tropopause for chemical integration. The meteorological fields for the model run are provided with the fifth-generation NCAR/Penn state mesoscale model (MM5), and the year of 1995 was selected for the MM5 simulation in this study. The chemical gas-phase mechanism in the model was initially developed by Stockwell (1986), and modified by updating the rate constants, introducing the effective photodissociation of ozone, incorporating the permutation reactions of organic peroxy radicals, and replacing the lumped NO₃ + N₂O₅ reaction rate expressions with the explicit ones (Ma et al., 2000). The revised chemical mechanism was well compared with the explicit NCAR's master mechanism using the trace gas concentrations observed at the China regional background atmospheric observatory as model initial conditions. The mechanism was further improved by adding acetone as a tracer into the model and including parameterization of heterogeneous reactions of N₂O₅ and NO₃ on sulfate aerosols (Ma et al., 2002a). The model implemented with this mechanism has been used for the study of tropospheric ozone over China (Ma et al., 2002a, b). In addition to updated anthropogenic surface emissions, natural NMVOC emissions, aircraft emissions and lightning NO_x sources are taken into account. The initial fields and lateral boundary condition for most chemical tracers are provided with a global chemical transport model for ozone and related chemical tracers (MOZART).

2.2. Emission inventories

The NO_x, CO and NMVOC emission inventories used are (i) emission estimates for the year 1995

from the Emission Database for Global Atmospheric Research (EDGAR v32; Olivier et al., 1999, 2002), (ii) regional emission inventory used in the Transport and Chemical Evolution over the Pacific (TRACE-P) program with emission estimates for the year 2000 (Streets et al., 2003) and (iii) national emission inventory used in the Chinese Ozone Research Programme (CORP) with emission estimates for the year 1995 (Bai, 1996). The reader is referred to the ACP paper of Ma and Van Aardenne (2004) for a detailed comparison of these emission inventories (<http://www.atmos-chem-phys.org/acp/4/877/>). The inventories are different in (i) year for which emissions are calculated, (ii) level of detail that is included, (iii) information source for emission factors and activity data, and (iv) method of distributing emissions to (1° × 1°) grid cells. The inventories share an important issue: due to the nature of emission factor calculations all inventories are known to be inaccurate representations of the emissions that have taken place in China over the year 1995.

The three emission inventories have been implemented into the model followed by a sensitivity run for each inventory. While different emission inventories are used for China, the EDGAR inventory is applied for other countries in the model domain in all simulations. Since all other model settings are kept constant, the difference in simulated tropospheric NO₂ will be due to various independent emission inventories for China. Ma and Van Aardenne (2004) investigated the difference in the concentrations of ozone and its precursors including NO_x over China due to the use of these emission inventories. The estimated NO_x emissions for China range from 11 to 19 Tg-NO₂ yr⁻¹ with large differences of up to 50% among the selected emission inventories, and these result in large differences of up to 200% in the simulated concentrations of NO_x on ground levels (Ma and van Aardenne, 2004).

2.3. GOME data

GOME is a passive remote sensing instrument on board the ERS-2 satellite, which was launched by the European Space Agency in April 1995 (European Space Agency (ESA), 1995). ERS-2 is in a sun-synchronous orbit, approximately 800 km above Earth, crossing the equator at 10:30 local time (LT) in the descending (N–S) node. The GOME instrument observes the atmosphere in

nadir view and global coverage is achieved every 3 days after 43 orbits with a footprint of 40 km latitude by 320 km longitude. It is designed to detect radiation reflected from the ground and scattered from the atmosphere, as well as extraterrestrial solar radiation, covering the wavelength range from 240 to 790 nm with the spectral resolution of 0.2–0.4 nm. From these measurements, trace gas total column amounts are retrieved utilizing the characteristic spectral absorption features. Although the main target species of GOME is ozone, other trace gases such as NO₂ can also be measured (Burrows et al., 1999).

In this study we use the most recent version (Version 2) of tropospheric NO₂ column data products that were created at the Institute of Environmental Physics (IUP), University of Bremen in the framework of European project POET (<http://nadir.nilu.no/poet/>). Satellite data are analyzed for tropospheric NO₂ in a four-step procedure. First, the NO₂ absorption averaged over all light paths contributing to the signal is determined using the differential optical absorption spectroscopy (DOAS) method in the 425–450 nm region (Richter and Burrows, 2002). In the second step, the stratospheric component is removed by subtracting the daily stratospheric NO₂ column simulated by the 3D CTM SLIMCAT (Chipperfield, 1999) for the time of the satellite overpass. To account for differences between model and measurement, the SLIMCAT data are scaled to the GOME data over a clean region (180°–210° longitude). In a third step, a cloud screening is applied removing those measurements with a cloud fraction of more than 0.2 as determined by the FRESCO algorithm (Koelemeijer, et al., 2001). The last step is the conversion of the tropospheric residual to a vertical tropospheric column by applying the pre-calculated air mass factors (AMF) with the radiative transfer model SCIATRAN (Rozanov et al., 1997). AMF prescribe an effective path of light in the troposphere and depend, in particular, on vertical distribution of the absorbing gas, aerosol and clouds in the troposphere, and on solar zenith angle and surface albedo. Different approaches and assumptions to evaluate AMF were used in different versions of data products of IUP. In particular, Version 1 data (see, e.g. Richter and Burrows, 2002; Lauer et al., 2002) were derived under simplified assumptions that all tropospheric NO₂ is homogeneously distributed in vertical below 1.5 km. The retrieval of Version 2 data is based on the use of

monthly AMF evaluated with NO₂ profiles from a run of the global model MOZART-2 model for 1997 (Horowitz et al., 2003).

GOME NO₂ measurement errors have been discussed in detail elsewhere (Richter and Burrows, 2002; Martin et al., 2002; Boersma et al. 2004). Briefly, GOME errors are dominated by clouds and air mass factor uncertainties. A rough estimate of the errors is an additive error of $0.5\text{--}1.0 \times 10^{15}$ molecules cm⁻² and a relative error of 40–60% over polluted areas. An additional uncertainty is introduced into the comparison by sampling and smoothing errors: GOME measurements have lower longitudinal resolution than the model which leads to apparent differences close to pollution hot spots (see Fig. 1). Also, the GOME orbital pattern and the cloud mask applied leads to non-uniform sampling of the NO₂ field, and can lead to less representative monthly averages, in particular in seasons and areas with high cloud coverage.

3. Results and discussions

3.1. General distribution pattern

Fig. 1 presents the geographical distribution of the tropospheric NO₂ column over China for July simulated with the model and retrieved from the GOME satellite data. Since both emission inventories EDGAR and CORP were developed for the year 1995 when the GOME data was not yet available, we use the GOME data for the year 1996 for comparison. The GOME data for the year of 2000 is also selected considering that the emission inventory TRACE-P was developed for this year. The GOME measurements in low and middle latitudes are always taken at the same LT (the northern mid-latitudes are crossed at about 10:45 LT). Correspondingly, we use the model output for each grid at 10:00–12:00 LT for comparison. One can see from the figure that high tropospheric NO₂ column densities (more than 4×10^{15} molecules cm⁻²) in polluted areas have been observed by GOME, and are reproduced by the model as well. The NO₂ column increases from 1996 to 2000 in the polluted regions around Beijing, Shanghai and Guangzhou have also been detected by GOME. However, the NO₂ column simulated with TRACE-P, which is the emission inventory for the year 2000, is lower than those simulated with EDGAR and CORP, which are the

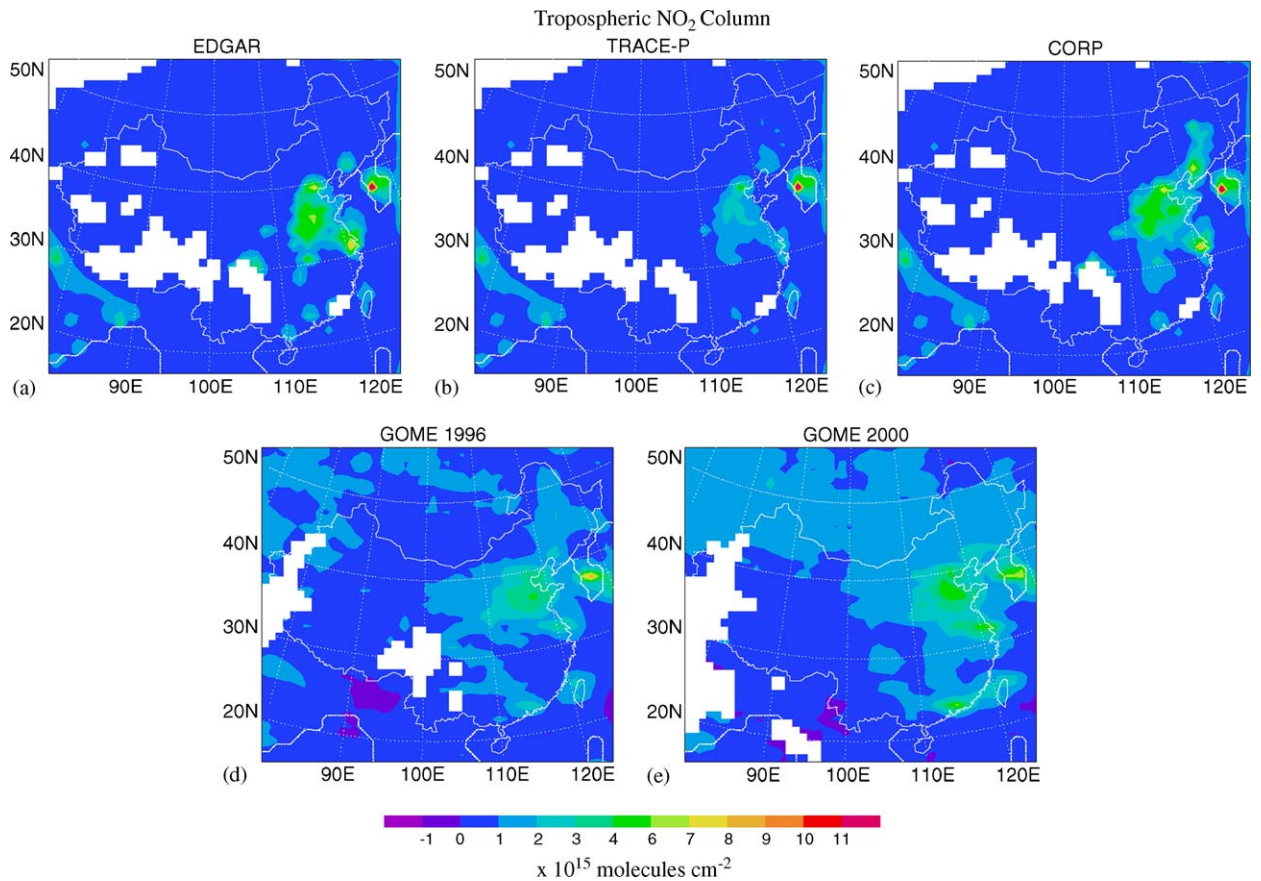


Fig. 1. Tropospheric NO₂ column densities in July calculated with the model using different emission inventories EDGAR (a), TRACE-P (b), and CORP (c) for the clear-sky conditions over the period 10:00–12:00 LT in comparison with the GOME data for the years 1996 (d) and 2000 (e). GOME data, which are provided with grid cells of 0.5° latitude × 0.5° longitude, have been interpolated to the model horizontal grids of 100 km × 100 km in the Lambert projection.

emission inventories for the year 1995. When using TRACE-P, the model underestimates the NO₂ column in comparison to the GOME measurements in both 1996 and 2000.

Missing values are found in Fig. 1 for both model results and GOME measurements because data taken under cloudy conditions have been removed. As described in Section 2.3 above, the GOME measurements with a cloud fraction of more than 0.2 as determined by the FRESCO algorithm were removed (see Koелеmeijer, et al., 2001). We also tried to use the cloud fraction of 0.2 as threshold to filter out the cloudy conditions for the model simulation and, as a result, missing values occurred for most regions in southern China. The cloud fraction seems rather difficult to predict precisely with current mesoscale models, and it appears to be overestimated by MM5 for the simulated period (see Ma et al., 2002a). Therefore, we use the

photodissociation coefficient of NO₂, i.e., $J\text{-NO}_2$, to separate clear and cloudy conditions in the present study. Specifically, a $J\text{-NO}_2$ value of $1.0 \times 10^{-2} \text{ s}^{-1}$ has been used as a threshold, with which the geographical distribution pattern of model data gaps matches that of the GOME 1996 data roughly. The sensitivity of comparison results to the threshold of $J\text{-NO}_2$ value will be tested below. Fig. 2 presents the tropospheric NO₂ to NO_x column density ratio under these clear-sky conditions over the period 10:00–12:00 LT. Only the simulation with the emission inventory of EDGAR is shown, as the influence of the difference in emission inventories on the ratio is negligible. As can be seen in the figure, the NO₂–NO_x ratio is higher in polluted areas, ranging from 0.5 to 0.7, due to higher ozone and peroxy radical concentrations favoring the shift in NO_x from NO to NO₂, while the effect of $J\text{-NO}_2$ value on the geographical distribution of the

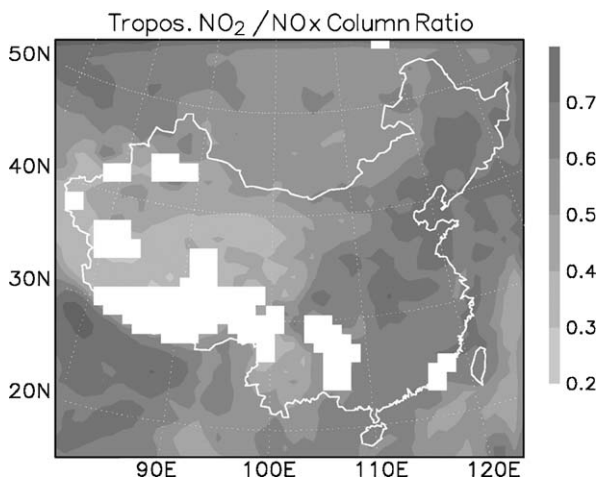


Fig. 2. Tropospheric NO_2 to NO_x column density ratio in July calculated with the model using the emission inventory EDGAR for clear-sky conditions over the period 10:00–12:00 LT.

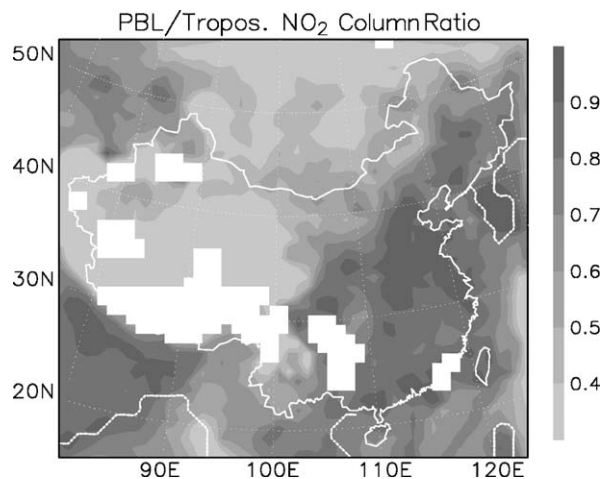


Fig. 3. PBL to tropospheric NO_2 column density ratio in July calculated with the model using the emission inventory EDGAR for clear-sky conditions over the period 10:00–12:00 LT.

NO_2 – NO_x ratio is not so significant under clear-sky conditions.

In this study, the model-simulated tropospheric NO_2 column density is an integration of the amount of NO_2 in each model layer from the ground to the thermal tropopause. For a sensitivity test, we also performed the integration of NO_2 up to the height of 150 mbar that was used in previous studies, e.g., by Kunhikrishnan et al. (2004). The variation in the NO_2 column (less than 5×10^{13} molecules cm^{-2}) was so small that it can be neglected, especially over polluted areas. The regional lifetime of NO_x estimated for China is about 14–21 h according to Kunhikrishnan et al. (2004), and hence a large part of NO_2 would be found in the regions near the NO_x sources. Fig. 3 presents the ratio of the planetary boundary layer (PBL) NO_2 column to the total tropospheric NO_2 column. It is shown that NO_2 accumulates predominantly in the PBL with a contribution of more than 90% over highly polluted areas.

3.2. Grid-to-grid and region-to-region comparisons

Scatter plots in Fig. 4 show grid-to-grid comparisons of the tropospheric NO_2 column densities calculated with the model using the emission inventories EDGAR, TRACE-P and CORP with the GOME data that have been interpolated into the model grids (Table 1). Different colors are used in the plots to specify the grids of different regions that are specified in Fig. 5. These regions include the

North of China (Beijing surrounding area) denoted with 'BJ', the Yangtze Delta (Shanghai surrounding area) denoted with 'SH', the Pearl River Delta (Guangzhou surrounding area) denoted with 'GZ', the western part of China denoted with 'WC', and the eastern part of China denoted with 'EC'. It is shown that with respect to the GOME measurements the model with TRACE-P underestimates the tropospheric NO_2 column density almost in all areas of China, and the model with EDGAR and CORP underestimates the tropospheric NO_2 column density in remote and most rural areas of China. EDGAR and CORP behave better in the North of China, but overestimate the NO_2 column in the Yangtze Delta and underestimate it in the Pearl River Delta. With respect to the correlation with the GOME measurements, the model with CORP appears to be the best and EDGAR the poorest when all the available data points in the model domain are included.

Fig. 6 presents region-to-region comparisons of mean tropospheric NO_2 column densities calculated with the model using different emission inventories with the GOME data. The average values of GOME 1996 are 3.1×10^{15} molecules cm^{-2} in the North of China where Beijing is located (1-BJ), 2.0×10^{15} molecules cm^{-2} in the Yangtze Delta where Shanghai is located (2-SH), 1.5×10^{15} molecules cm^{-2} in the Pearl River Delta where Guangzhou is located (3-GZ), 0.8×10^{15} molecules cm^{-2} in the western part of China (4-WC), and 1.1×10^{15} molecules cm^{-2} in the

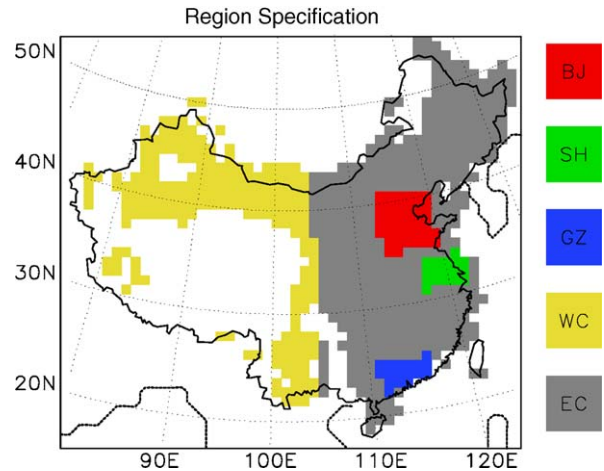
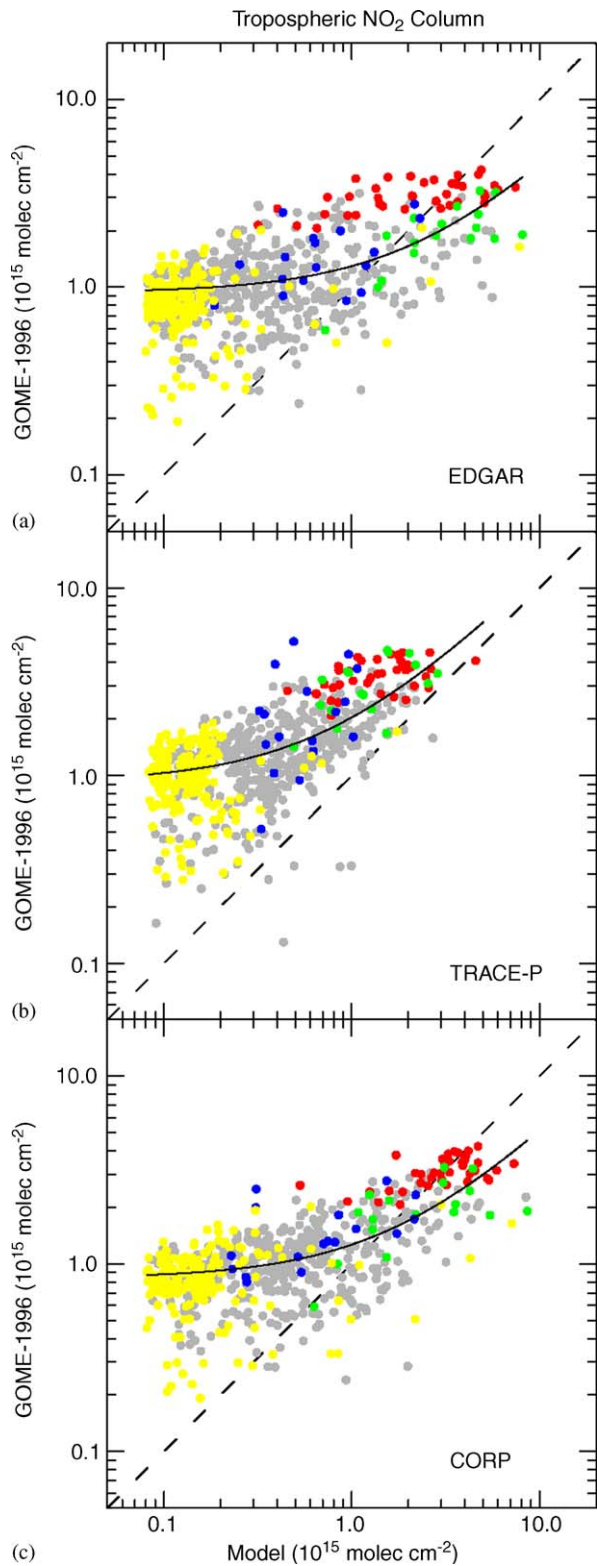


Fig. 5. Specification of different regions in China selected for comparisons. The North of China (35–42°N, 112–120°E) where Beijing is located is shown in red (denoted with ‘BJ’), the Yangtze Delta (28–35°N, 117–123°E) where Shanghai is located is shown in green (denoted with ‘SH’), the Pearl River Delta (22–25°N, 111–117°E) where Guangzhou is located is shown in blue (denoted with ‘GZ’), the western part of China (to the west of 105°E) is shown in yellow (denoted with ‘WC’), and the rest of China mainland are shown in gray (denoted with ‘EC’).

rest of China mainland (5-EC). All the magnitudes of NO₂ columns are represented by the ratios of their values to the GOME 1996 values in the same regions. As found above, the model with TRACE-P underestimates the GOME measurements in 2000 by more than 50% for all the regions. The tropospheric NO₂ column is simulated well (within 6–12% deviation) in the case of 1-BJ, overestimated (by 43–77%) in the case of 2-SH, and underestimated (by 43–44%) in the case of 3-GZ by the model with EDGAR and CORP when compared to the GOME measurements in 1996. The model underestimates the GOME measurements in remote and less-polluted rural regions of China (69–84% and 33–64% in the cases 4-WC and 5-EC, respectively) no matter what emission inventory is

←
Fig. 4. Scatter plots of tropospheric NO₂ column densities calculated with the model using different emission inventories EDGAR (a), TRACE-P (b) and CORP (c) versus the GOME data in July for the years of 1996 (a, c) and 2000 (b). The color of the symbols corresponds to the color of the individual regions in Fig. 5. Solid curves refer to a linear regression with the data points of all the regions. Note that logarithmic coordinates are used and thus the linear regression looks curvilinear in the plots. A summary of comparison statistics is given in Table 1. All data have the same units of 10¹⁵ molecules cm⁻².

Table 1
Comparison statistics for the data points in Fig. 4

	Samples	r^2	Slope	Intercept	Bias (%)
1-BJ					
GOME 1996/EDGAR	39	0.237	0.150	2.70	-12
GOME 2000/TRACE-P	39	0.186	0.367	2.84	-56
GOME1996/CORP	39	0.253	0.197	2.46	6
2-SH					
GOME 1996/EDGAR	17	0.326	0.204	1.26	77
GOME 2000/TRACE-P	17	0.238	0.715	2.01	-55
GOME1996/CORP	17	0.147	0.132	1.60	43
3-GZ					
GOME 1996/EDGAR	17	0.309	0.542	1.05	-43
GOME 2000/TRACE-P	17	0.099	1.572	1.36	-74
GOME1996/CORP	17	0.249	0.449	1.13	-44
4-WC					
GOME 1996/EDGAR	186	0.059	0.121	0.828	-75
GOME 2000/TRACE-P	182	0.017	0.338	0.960	-84
GOME1996/CORP	186	0.063	0.119	0.822	-69
5-EC					
GOME 1996/EDGAR	424	0.128	0.211	0.985	-45
GOME 2000/TRACE-P	420	0.283	0.792	0.995	-64
GOME1996/CORP	424	0.3336	0.342	0.856	-33
All the regions					
GOME 1996/EDGAR	683	0.360	0.361	0.935	-41
GOME 2000/TRACE-P	675	0.472	1.124	0.920	-67
GOME1996/CORP	683	0.509	0.431	0.835	-31

Note: we use the linear equation $Y = A \times X + B$, where X , Y , A and B refer to the model NO_2 column, GOME NO_2 column, slope and intercept, respectively. Bias = $(X_{\text{mean}} - Y_{\text{mean}}) / Y_{\text{mean}} \times 100$.

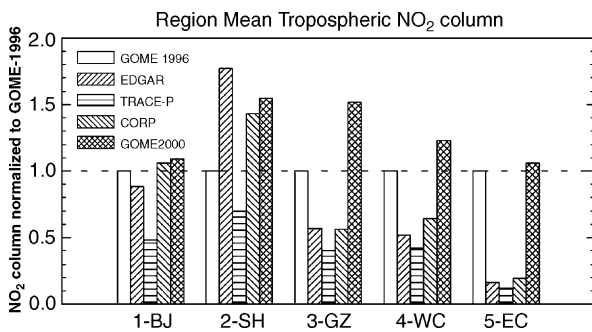


Fig. 6. Normalized tropospheric NO_2 columns for the regions BJ, SH, GZ, WC and EC that are defined in Fig. 5. The mean model NO_2 columns for emissions inventories EDGAR, TRACE-P and CORP and the mean GOME NO_2 column for the year 2000 are scaled to the mean GOME NO_2 column for 1996 in the same region.

used. Comparisons of the GOME 1996 and 2000 data show that the NO_2 column increases during the period in all the regions, even including western

China. The reason for the apparent NO_2 increase in the remote region could be either due to real differences in the NO_2 fields, or to errors in the retrieval, which are estimated to be of the same order of magnitude (see Section 2.3).

3.3. Sensitivity tests

As described in Section 3.1, we use a $J\text{-NO}_2$ value of $1.0 \times 10^{-2} \text{ s}^{-1}$ as threshold to distinguish between the clear-sky and cloudy conditions for the model results. Since selection of this $J\text{-NO}_2$ value is more or less arbitrary, we performed calculations using different $J\text{-NO}_2$ values as threshold to investigate the sensitivity of our results to the approach used in the present study. Fig. 7 presents the changes in the model-to-GOME 1996 tropospheric NO_2 column ratio as a function of $J\text{-NO}_2$ threshold. The Beijing surrounding area (BJ), which is a representative of highly polluted regions, and eastern China rural areas (EC), which belong to less polluted regions,

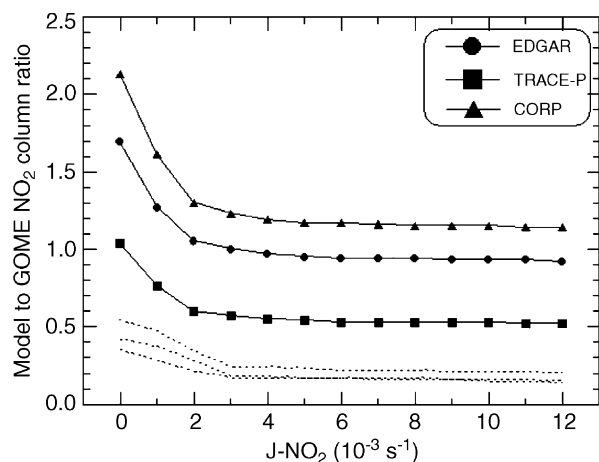


Fig. 7. Changes in the model-to-GOME ratio of region mean tropospheric NO_2 columns as a function of $J\text{-NO}_2$ threshold that is used for the selection of model results for the clear-sky conditions. Solid and dotted lines are the results for the Beijing surrounding area (BJ) and eastern China rural areas (EC), respectively, which are specified in Fig. 5. The $J\text{-NO}_2$ value of $10 \times 10^{-3} \text{ s}^{-1}$ has been used as a threshold for the present study.

are chosen for presentation. It can be seen that for a wide range of thresholds, i.e., $J\text{-NO}_2$ larger than $2\text{--}3 \times 10^{-3} \text{ s}^{-1}$, the changes in the model-to-GOME NO_2 column ratio are very small (within 10%). Only when the threshold changes from $2\text{--}3 \times 10^{-3}$ to 0 s^{-1} , the ratio changes significantly by up to 200%, but these $J\text{-NO}_2$ values represent cloudy conditions and hence cannot be chosen as the threshold.

4. Conclusions

We have compared tropospheric NO_2 columns over China simulated with a regional model using different emission inventories EDGAR, TRACE-P and CORP, respectively, with measurements from the GOME satellite. The model generally reproduces high tropospheric NO_2 column densities in polluted areas of China that have been observed by GOME. However, the model simulations do not agree with the GOME measurements in a quantitative sense for some regions. We performed linear regressions with the NO_2 column densities available from GOME, Y , and the model, X , of each grid cell in selected regions. For all the region of China, comparison statistics are $Y = 0.361 \times X + 0.935$ with $r^2 = 0.360$ and bias = -41% for EDGAR, $Y = 1.124 \times X + 0.920$ with $r^2 = 0.472$ and

bias = -67% for TRACE-P, and $Y = 0.431 \times X + 0.835$ with $r^2 = 0.509$ and bias = -31% for CORP. Our study is the first to look at the regional distribution of NO_x emissions in China, while previous studies always treated larger areas (China or Asia).

In the polluted regions around Beijing, Shanghai and Guangzhou, NO_2 column increases from 1996 to 2000 have been detected by GOME. However, the NO_2 column simulated with TRACE-P, which is the emission inventory for the year 2000, is lower than those simulated with EDGAR and CORP, which are emission inventories for the year 1995. We have found that TRACE-P underestimates the tropospheric NO_2 column density in all the regions with respect to the GOME measurements (by more than 50%). There have been several studies using CO observations from aircraft during TRACE-P and from satellite which have come to the same conclusion, which is that Chinese emissions in the TRACE-P inventory are too low (e.g., Palmer et al., 2003; Carmichael et al., 2003; Allen et al., 2004; Heald et al., 2004). EDGAR and CORP appear to behave well for the model simulations in the North of China (within 15% deviations), but poorer for the model simulations in the Yangtze Delta (overestimate by 45–75%) and in the Pear River Delta (underestimate by 45%). All the emission inventories used underestimate the tropospheric NO_2 column density in remote and less-polluted rural areas significantly. However, the uncertainties in estimated difference are large due to larger relative errors of GOME measurements over these regions. On the other hand, a recent study of Wang et al. (2004) used observations of CO and NO_y over China and found that in addition to increasing the TRACE-P emissions they had to invoke a very large source of NO_x from soils because of fertilizers and release of NO_x from human and animal wastes to bring model and measurements into agreement.

In this study we use the $J\text{-NO}_2$ value as threshold to select the clear-sky conditions for the model results. Although the definition of $J\text{-NO}_2$ threshold value is more or less arbitrary, sensitivity test show that this would not affect our result so much. On the other hand, in order to filter out cloudy conditions GOME measurements use cloud fraction as threshold, which seems rather difficult to observe by satellites and predict precisely with current meso-scale models. The GOME NO_2 data analysis uses a priori profile information taken from a MOZART model run, which in turn is based on the EDGAR

emissions, albeit on a coarse spatial scale. This could have an impact on the comparison between model and satellite measurement, although the retrieval is affected not by the absolute amount but only by the vertical distribution of the NO₂. According to Velders et al. (2001), the measured tropospheric NO₂ amounts derived from GOME data are a factor of 2–3 larger than those calculated by the MOZART model for Asia. In the study of Martin et al. (2003), their global model a posteriori estimate agrees closely with the EDGAR 3.0 bottom-up inventory, but there are significant differences in some regions including Asia.

All the emission estimates we use are based on the yearly statistical data that have no information on seasonal variations. Seasonal variation in the emissions can be significant at least in the northern part of China due to heating in winter. Over Beijing for instance, the emissions in July are estimated to be 70% of those averaged over a year. Complete comparisons of model simulated tropospheric NO₂ columns with GOME data should be made for different months and different years. The difference in the total of NO_x emissions over China is 50% among the three emission inventories used in this study, and the difference between EDGAR and TRACE-P is less than 10%. However, larger discrepancy in the tropospheric NO₂ columns over different regions between the model simulations and the GOME measurements are found in this study. This highlights the need for spatially high-resolved NO_x emission inventories with good accuracy as they have a large impact on NO_x concentrations predicted by models. Measurements from satellite instruments such as GOME, and in the future the Scanning Imaging Absorption Spectrometer for Atmospheric Chartography (SCIAMACHY) on board ENVISAT and the Ozone Monitoring Instrument (OMI) on board Aura, which both provide better spatial resolution, can help to identify deficiencies in existing emission inventories and might also be used to improve such estimates by inverse modeling.

Acknowledgments

J. Ma was supported by the Natural Science Foundation of China under the projects 40375040 and 40433008. GOME lv1 data was provided by ESA through DLR/DFD.

References

- Allen, D., Pickering, K., Fox-Rabinovitz, M., 2004. Evaluation of pollutant outflow and CO sources during TRACE-P using model-calculated, aircraft-based, and measurements of pollution in the troposphere (MOPITT)-derived CO concentrations. *Journal of Geophysical Research* 109, D15S03.
- Bai, N.B., 1996. The emission inventory of CO₂, SO₂, and NO_x in China. In: Zhou, X.J. (Ed.), *The Atmospheric Ozone Variation and Its Effect on the Climate and Environment in China*. Meteorological Press, Beijing, pp. 145–150 (in Chinese).
- Beirle, S., Platt, U., Wenig, M., Wagner, T., 2003. Weekly cycle of NO₂ by GOME measurements: a signature of anthropogenic sources. *Atmospheric Chemistry and Physics* 3, 2225–2232.
- Bey, I., Jacob, D.J., Yantosca, R.M., Logan, J.A., Yantosca, R.M., 2001. Asian chemical outflow to the Pacific in spring: origins, pathways, and budgets. *Journal of Geophysical Research* 106, 23097–23114.
- Boersma, K.F., Eskes, H.J., Brinksma, E.J., 2004. Error analysis for tropospheric NO₂ retrieval from space. *Journal of Geophysical Research* 109, D04311.
- Bradshaw, J., Davis, D., Grodzinsky, G., Smyth, S., Newell, R., Sandholm, S., Liu, S., 2000. Observed distributions of nitrogen oxides in the remote free troposphere from the NASA global tropospheric experiment programs. *Review of Geophysics* 38, 61–116.
- Burrows, J.P., Weber, M., Buchwitz, M., Rozanov, V.V., Ladstätter-Weissenmayer, A., Richter, A., DeBeek, R., Hoogen, R., Brmstedt, K., Eichmann, K.U., 1999. The global ozone monitoring experiment (GOME): mission concept and first scientific results. *Journal of Atmospheric Science* 56, 151–175.
- Carmichael, G.R., et al., 2003. Regional-scale chemical transport modeling in support of the analysis of observations obtained during the TRACE-P experiment. *Journal of Geophysical Research* 108 (D21), 8823.
- Chipperfield, M.P., 1999. Multiannual simulations with a three-dimensional chemical transport model. *Journal of Geophysical Research* 104, 1781–1806.
- Crutzen, P.J., 1979. The role of NO and NO₂ in the chemistry of the troposphere and stratosphere. *Annual Review of Earth Planet Science* 7, 443–472.
- Edwards, D.P., Lamarque, J.-F., Attié, J.-L., Emmons, L.K., Richter, A., Cammas, J.-P., Gille, J.C., Francis, G.L., Deeter, M.N., Warner, J., Ziskin, D.C., Lyjak, L.V., Drummond, J.R., Burrows, J.P., 2003. Tropospheric ozone over the tropical Atlantic: a satellite perspective. *Journal of Geophysical Research* 108 (D8), 4237.
- Environmental Protection Agency (EPA), 2000. Air quality index—a guide to air quality and your health. Washington, DC, 20460. EPA-454/R-00-005.
- European Space Agency (ESA), 1995. GOME global ozone measuring experiment users manual. ESA SP-1182, ESA/ESTEC, Noordwijk, The Netherlands, ISBN: 92-9092-327-x.
- Garg, A., Shukla, P.R., Bhattacharya, S., Dadhwal, V.K., 2001. Sub-region (district) and sector level SO₂ and NO_x emissions for India—assessment of inventories and mitigation flexibility. *Atmospheric Environment* 35, 703–713.

- Heald, C.L., Jacob, D.J., Jones, D.B.A., Palmer, P.I., Logan, J.A., Streets, D.G., Sachse, G.W., Gille, J.C., Hoffman, R.N., Nehr Korn, T., 2004. Comparative inverse analysis of satellite (MOPITT) and aircraft (TRACE-P) observations to estimate Asian sources of carbon monoxide. *Journal of Geophysical Research* 109, D23306.
- Horowitz, L.W., Horowitz, L.W., Walters, S., Mauzerall, D.L., Emmons, L.K., Rasch, P.J., Granier, C., Tie, X., Lamarque, J.-F., Schultz, M.S., Tyndall, G.S., Orlando, J.J., Brasseur, G.P., 2003. A global simulation of tropospheric ozone and related tracers: description and evaluation of MOZART, version 2. *Journal of Geophysical Research* 108 (D24), 4784.
- Kato, N., Akimoto, H., 1992. Anthropogenic emissions of SO₂ and NO_x in Asia: emissions inventories (plus errata). *Atmospheric Environment* 26A, 2997–3017.
- Koelemeijer, R.B.A., Stammes, P., Hovenier, J.W., de Haan, J.F., 2001. A fast method for retrieval of cloud parameters using oxygen A band measurements from the global ozone monitoring experiment. *Journal of Geophysical Research* 106, 3475–3490.
- Kononov, I.B., Beekmann, M., Vautard, R., Burrows, J.P., Richter, A., Nüß, H., Elansky, N., 2005. Comparison and evaluation of modelled and GOME measurement derived tropospheric column NO₂ column over Western and Eastern Europe. *Atmospheric Chemistry and Physics* 5, 169–190.
- Kunhikrishnan, T., Lawrence, M.G., v. Kuhlmann, R., Richter, A., Ladstätter-Weissenmayer, A., Burrows, J.P., 2004. Analysis of tropospheric NO_x over Asia using the model of atmospheric transport and chemistry (MATCH-MPIC) and GOME-satellite observations. *Atmospheric Environment* 38, 581–596.
- Lauer, A., Dameris, M., Richter, A., Burrows, J.P., 2002. Tropospheric NO₂ column: a comparison between model and retrieved data from GOME measurements. *Atmospheric Chemistry and Physics* 2, 67–87.
- Lee, D.S., Köhler, I., Grobler, E., Rohrer, F., Sausen, R., Gallardo-Klenner, L., Olivier, J.G.J., Dentener, F.J., Bouwman, A.F., 1997. Estimation of global NO_x emissions and their uncertainties. *Atmospheric Environment* 31, 1735–1749.
- Lelieveld, J., Dentener, F.J., Peters, W., Krol, M.C., 2004. On the role of hydroxyl radicals in the self-cleansing capacity of the atmosphere. *Atmospheric Chemistry and Physics* 4, 2337–2344.
- Leue, C., Wenig, M., Wagner, T., Platt, U., Jähne, B., 2001. Quantitative analysis of NO_x emissions from GOME satellite image sequences. *Journal of Geophysical Research* 106, 5493–5505.
- Logan, J.A., Prather, M.J., Wofsy, S.C., MeElroy, M.B., 1981. Tropospheric chemistry: a global perspective. *Journal of Geophysical Research* 86, 7210–7254.
- Ma, J., van Aardenne, J.A., 2004. Impact of different emission inventories on simulated tropospheric ozone over China: a regional chemical transport model evaluation. *Atmospheric Chemistry and Physics* 4, 877–887.
- Ma, J., Li, W.L., Zhou, X.J., 2000. Improvements of RADMI gas phase chemical mechanism. *Journal of Environmental Science and Health A* 35, 1931–1939.
- Ma, J., Liu, H.L., Hauglustaine, D., 2002a. Summertime tropospheric ozone over China simulated with a regional chemical transport model, 1. Model description and evaluation. *Journal of Geophysical Research* 107 (D22), 4660.
- Ma, J., Zhou, X.J., Hauglustaine, D., 2002b. Summertime tropospheric ozone over China simulated with a regional chemical transport model, 2. Source contributions and budget. *Journal of Geophysical Research* 107 (D22), 4612.
- Martin, R.V., Chance, K., Jacob, D.J., Kurosu, T.P., Spurr, R.J.D., Bucsela, E., Gleason, J.F., Palmer, P.I., Bey, I., Fiore, A.M., Li, Q., Yantosca, R.M., Koelemeijer, R.B.A., 2002. An improved retrieval of tropospheric nitrogen dioxide from GOME. *Journal of Geophysical Research* 107 (D20), 4437.
- Martin, R.V., Jacob, D.J., Chance, K., Kurosu, T.P., Palmer, P.I., Evans, M.J., 2003. Global inventory of nitrogen oxide emissions constrained by space-based observations of NO₂ columns. *Journal of Geophysical Research* 108 (D17), 4537.
- Müller, J.-F., Stavrou, T., 2005. Inversion of CO and NO_x emissions using the adjoint of the IMAGES model. *Atmospheric Chemistry and Physics* 5, 1157–1186.
- Olivier, J.G.J., Bloos, J.P.J., Berdowski, J.J.M., Visschedijk, A.J.H., Bouwman, A.F., 1999. A 1990 global emission inventory of anthropogenic sources of carbon monoxide on 1° × 1° developed in the framework of EDGAR/GEIA. *Chemosphere: Global Change Science* 1, 1–17.
- Olivier, J.G.J., Peters, J.A.H.W., Bakker, J., Berdowski, J.J.M., Visschedijk, A.J.H., Bloos, J.P.J., 2002. Applications of EDGAR: emission database for global atmospheric research. Report no.: 410.200.051. RIVM, The Netherlands.
- Palmer, P.I., Jacob, D.J., Jones, D.B.A., Heald, C.L., Yantosca, R.M., Logan, J.A., Sachse, G.W., Streets, D.G., 2003. Inverting for emissions of carbon monoxide from Asia using aircraft observations over the western Pacific. *Journal of Geophysical Research* 108 (D21), 8828.
- Parrish, D.D., Trainer, M., Williams, E.J., Fahey, D.W., Hübler, G., Eubank, S., Liu, S., Murphy, P.C., Albritton, D.L., Fehsenfeld, F.C., 1986. Measurements of the NO_x-O₃ photostationary state at Niwot Ridge, Colorado. *Journal of Geophysical Research* 91, 5361–5370.
- Richter, A., Burrows, J.P., 2002. Retrieval of tropospheric NO₂ from GOME measurements. *Advance in Space Research* 29, 16,673–16,683.
- Richter, A., Burrows, J.P., Nüß, H., Granier, C., Niemeier, U., 2005. Increase in tropospheric nitrogen dioxide over China observed from space. *Nature* 437, 129–132.
- Ridley, B.A., Madronich, S., Chatfield, R.B., Walega, J.G., Shetter, R.E., Carroll, M.A., Montzka, D.D., 1992. Measurements and model simulations of the photostationary state during the Mauna Lao observatory photochemistry experiment: implication for radical concentrations and ozone production and loss rates. *Journal of Geophysical Research* 97, 10,375–10,388.
- Rozañov, V., Diebel, D., Spurr, R.J.D., Burrows, J.P., 1997. GOMETRAN: a radiative transfer model for the satellite project GOME—the plane parallel version. *Journal of Geophysical Research* 102, 16,683–16,695.
- Schaub, D., Weiss, A.K., Kaiser, J.W., Petritoli, A., Buchmann, B., Burrows, J.P., 2005. A transboundary transport episode of nitrogen dioxide as observed from GOME and its impact in the Alpine region. *Atmospheric Chemistry and Physics* 5, 23–37.
- Solomon, S., Portmann, R.W., Sanders, R.W., Daniel, J.S., Madsen, W., Bartram, B., Dutton, E.G., 1999. On the role of nitrogen dioxide in the absorption of solar radiation. *Journal of Geophysical Research* 104, 12,407–12,458.

- Stockwell, W.R., 1986. A homogeneous gas-phase mechanism for use in a regional acid deposition model. *Atmospheric Environment* 20, 1615–1632.
- Streets, D.G., Waldhoff, S.T., 2000. Present and future emissions of air pollutants in China: SO₂, NO_x, and CO. *Atmospheric Environment* 34, 363–374.
- Streets, D.G., Bond, T.C., Carmichael, G.R., Fernandes, S.D., Fu, Q., He, D., Klimont, Z., Nelson, S.M., Tsai, N.Y., Wang, M.Q., Woo, J.-H., Yarber, K.F., 2003. An inventory of gaseous and primary aerosol emissions in Asia in the year 2000. *Journal of Geophysical Research* 108 (D21), 8809.
- Thompson, A.M., 1992. The oxidizing capacity of Earth's atmosphere: probable past and future changes. *Science* 256, 1157–1165.
- van Aardenne, J.A., Carmichael, G.R., Levy II, H., Streets, D., Hordijk, L., 1999. Anthropogenic NO_x emission in Asia in the period 1990–2020. *Atmospheric Environment* 33, 633–646.
- Velders, G.J.M., Granier, C., Portmann, R.W., Pfeilsticker, K., Wenig, M., Wagner, T., Platt, U., Richter, A., Burrows, J.P., 2001. Global tropospheric NO₂ column distributions: comparing three-dimensional model calculations with GOME measurements. *Journal of Geophysical Research* 106, 12,643–12,660.
- Wang, Y.X., McElroy, M.B., Wang, T., Palmer, P.I., 2004. Asian emissions of CO and NO_x: constraints from aircraft and Chinese station data. *Journal of Geophysical Research* 109, D24304.